FIRE RESISTANCE AND ASSOCIATED FAILURE MODES OF AXIALLY RESTRAINED HOLLOW CORE SLABS

Thomas Thienpont[1*], Wouter De Corte[1], Robby Caspeele[1], Ruben Van Coile[1]

[1] Department of Structural Engineering and Building Materials, Ghent University, Ghent, Belgium
Postal address: Technologiepark-Zwijnaarde 60, B-9052 Gent, Belgium
* Corresponding author: Thomas.Thienpont@UGent.be

ABSTRACT

When a severe fire occurs in the central part of a large hollow core slab floor, the thermal expansion of the affected floor members will be highly restrained by the stiffness of the surrounding structure. The present paper presents the development of a numerical model to evaluate the structural performance of precast concrete hollow core slabs exposed to fire, taking into account the interaction with the surrounding structure and how it affects the fire resistance and failure mode. The performance of the model is validated against fire tests reported in literature. Subsequently the model is employed to evaluate the influence of various degrees of restraint on the fire resistance of three hollow core slab sections, with depths ranging from 200 mm to 500 mm. The results indicate that restrained thermal expansion can significantly enhance the fire resistance of concrete hollow core slabs with low span-to-depth ratios. Conversely, in hollow core slabs with a high span-to-depth ratio, the restraint provided by the surroundings can considerably impair the fire performance. Additionally, it is shown that the failure mode of hollow core slabs can change from ductile bending failure to a brittle shear failure mode in the presence of axially restraining boundary conditions.

KEYWORDS

fire resistance, restrained expansion, hollow core slab, finite element analysis, failure modes

1 INTRODUCTION

Precast concrete hollow core (HC) slabs are nowadays intensively used in many countries, with the annual global production of these elements reaching 50 million m² [1]. They offer a considerable scope for new demands in the domain of future building construction: structural efficiency, long spans up to more than 20 m in combination with shallower construction depths. Furthermore, their semi-automatic manufacturing process results in a reduced use of materials, energy and production waste [2].

When exposed to a severe fire, the load-carrying capacity of concrete HC slabs decreases with time due to the degradation of the material's mechanical properties at elevated temperatures and due to damage caused by thermal stresses. The structural response of HC slabs exposed to fire has been the subject of numerous studies, and over the years a large body of fire tests on both single members and hollow core floor assemblies have been performed. In the majority of these tests, simply supported boundary conditions are employed, in which the members can expand freely in all directions. In practice however, the thermal expansion of fire exposed HC members will be restrained by the stiffness of the surrounding structure, especially when the fire occurs in the central part of a large hollow core slab floor. As a result of this restrained expansion, compressive forces develop inside the member, which strongly affect its structural behaviour and fire resistance. Experimental tests at ambient temperature have shown that the load-carrying capacity of restrained HC slabs can be enhanced significantly due to formation of compression arching action (CAA) in the webs of the slabs [3]. A similar effect can occur in fire exposed HC slabs, where CAA could be activated due to the restrained thermal expansion, resulting in a higher flexural capacity then accounted for based on classic small-deformation structural analysis calculations. The relevance of this effect was already recognised in 1965 [4], and it was suggested that restraint of the thermal expansion might significantly increase the fire resistance of HC slabs. This hypothesis was further studied by Dotreppe & Franssen in a series of fire tests on double span HC floors [5,6]. Herein, the outward expansion of the HC slabs in the floor assembly was restrained by a set of reinforced concrete edge beams and two cold steel bars on both sides of the floor, anchored to the edge beams. The results indicate that even a small degree of axial restraint can positively affect the shear capacity of fire exposed HC slabs. Consequently, axial restraint could delay or even prevent a structural failure and collapse of a hollow core floor in case of fire. A similar observation was reported by Fellinger et al. [7,8], based on fire tests on double rib slab specimens, and a detailed numerical model. They concluded that restraining the axial thermal expansion significantly improves the fire resistance of HC slabs with respect to shear and anchorage failure. More recently, Shakya & Kodur [9,10] performed fire tests on a restrained and a simply supported full-scale HC slab, and reported a 30 minute increase in fire resistance due to the restrained thermal expansion in the restrained specimen.

Although the previously mentioned studies highlight the beneficial effects of restrained thermal expansion on the fire performance of HC slabs, one should be cautious to generalize these positive effects for all shapes and sizes. Furnace tests have evidenced the possible formation of CAA and a corresponding enhanced performance, but always in members with relatively short spans. This is mainly due to the size limitations of commonly used test furnaces, which typically measure 4.27 m (14 ft) to 5.18 m (17 ft) in length [11]. As the beneficial effects of CAA strongly decrease with increasing span-to-depth ratio, it is not guaranteed that this effect will enhance the fire resistance of HC slabs with more realistic span lengths. Indeed, a study on reinforced concrete beams has shown that fire induced restraint can have a negative effect on the fire resistance in members with a high span-to-depth ratio [12]. To the knowledge of the authors, no restrained fire tests on HC slabs with a high span-to-depth ratio ($L/h > 20$) are reported in literature. In practice however, span-to-depth ratios of $L/h = 35$ are not uncommon, and it’s currently unclear to what extent restrained expansion can improve the fire resistance of HC slabs in these real-scale applications.

Furthermore, in the study by Shakya & Kodur [9,10], it was shown that the presence of axial restraints can also influence the failure mode of HC slabs. Based on the observed crack patterns from fire tests of two HC slabs with a height of 200 mm, it was concluded that the restrained slab failed due to excessive cracking and crushing of concrete at the mid-span, whereas the failure mode of the unrestrained sample was identified as flexural bending. In a similar set of experiments, on the influence of axial restraints in HC slabs (height of 320 mm) at ambient conditions, it was shown that restrained HC slabs can fail due to a brittle shear-tension failure, while the cracking pattern in the unrestrained specimen indicated a flexural failure mode [3].

Thus far, only very few studies have focused on the effect of restrained thermal expansion in fire exposed HC slabs with span lengths typically employed in real structures, and on the determination of the conditions under which this effect is actually beneficial. Furthermore, a better understanding of how various degrees of restrained thermal expansion during a fire scenario can alter the failure mode of HC slabs is needed. This is especially the case for deep HC slabs, as no restrained tests have been reported on members with a height taller than 200 mm. This contribution focusses on studying these effects by means of a detailed 3D numerical model, which is validated against tests available in literature. The model is employed in an extensive parametric study in order to assess the effect of various degrees of axial restraint on the fire resistance and failure mode of three types of HC slabs, ranging in depth from 200 mm to 500 mm, and span-to-depth ratios ranging from L/h = 25 to L/h = 35.

2 NUMERICAL MODEL

To investigate the influence of various degrees of axial restraint on the structural behaviour and failure mode of fire exposed HC slabs, a numerical model is developed using the finite element software Abaqus [13]. The numerical modeling approach consists of a two-step sequentially coupled analysis. Firstly, a transient heat transfer analysis is performed to obtain the temperature distribution inside the member at each point in time. Subsequently, this temperature data is used as input for a mechanical thermal-stress analysis to evaluate the structural behaviour. First, the details of the sequentially coupled analysis are discussed in Section 2.1 and 2.2. Subsequently, in Section 2.3, the performance of the numerical model is validated against experimental results reported in literature.

2.1 HEAT TRANSFER ANALYSIS

To obtain the temperature evolution inside the HC slab, a 3D heat transfer analysis is performed. The concrete is modelled using 8-noded hexahedral (brick) heat transfer elements (DC3D8) with an average size of 25 mm. The prestressing steel is assumed not to influence the temperature calculations, and the prestressing strands are therefore not included in the heat transfer analysis [14]. The strand temperatures are assumed equal to the temperature of the surrounding concrete, which is a common assumption in structural fire calculations, see for example [15–19]. The temperature dependent material properties (thermal conductivity, specific heat and density) governing the heat transfer inside the concrete and the boundary conditions governing the heat transfer at the concrete-air interface are taken from EN 1992-1-2:2004 [19] and EN 1991-1-2:2002 [20] respectively. At the fire exposed surfaces, a concrete emissivity $\varepsilon_c = 0.7$ and convective heat transfer coefficient $\alpha_c = 25$ W/m²K are used. At the unexposed side, the convection coefficient is taken as $\alpha_c = 9$ W/m²K, assuming it contains the effects of heat transfer by radiation. Additionally, the heat transfer inside the hollow cores is considered by using the cavity radiation function in Abaqus, assuming a concrete emissivity $\varepsilon_c = 0.7$. This allows for radiation energy to be transferred between the (hotter) bottom surface and the (colder) upper surface of the hollow cores, and results in faster heating of the upper regions of the slab compared to solid slabs.

2.2 STRUCTURAL ANALYSIS

Subsequently, based on the calculated temperature field, a structural analysis is performed. Herein, 8-noded hexahedral (brick) elements (C3D8R) with reduced integration and 2-noded linear truss elements (T3D2) are used to model the concrete and steel prestressing strands, respectively. Assuming perfect bond, the prestressing strands are embedded within the concrete element, using the embedded constraint option in Abaqus. The constitutive models for the temperature-dependent stress-strain behaviour of both the concrete and prestressing steel are taken from EN 1992-1-2:2004 [19]. The Concrete Damage Plasticity (CDP) model of Abaqus is adopted to simulate multi-axial behaviour of concrete, which allows capturing both crushing and cracking failure of the material. The uniaxial tensile behaviour of concrete, is modelled using a stress-crack opening relation. Herein, the stress-crack opening function and the temperature dependent strength retention values are based on *fib* Model Code 2010 [21] and EN 1992-1-2 [19], respectively. The area under each stress-crack opening curve corresponds to the fracture energy, which is calculated based on *fib* Model Code 2010 and assumed constant with increasing temperatures. This is a common assumption in the numerical modelling of concrete exposed to fire [7,18,22], since there is very limited test data available on the fracture energy of concrete at high temperatures. Lastly, the temperature dependent thermal expansion of concrete and steel is also modelled in accordance with EN 1992-1-2:2004 [19].

In the mechanical analysis, the Abaqus/Explicit solver is employed, as it allows for efficient modeling of highly nonlinear static (quasi-static) problems. The mechanical analysis consist of two steps. In the first step, the prestress, self-weight and line loads are applied. Subsequently, the structural response of the HC slab under fire exposure is simulated by mapping the results from the heat transfer model onto the mechanical model. The output parameters from the analyses include sectional temperatures, reaction forces, deflections, stresses and strains at each time step. By analysing the plastic strains, the development of cracks during the fire exposure can be studied. Note that the numerical model does not track crack growth explicitly. Rather, the development of cracks can be indicated by areas of high plastic strains.

In the analysis, failure of the specimen is defined as the point in time where the load-carrying capacity shows a sudden irrecoverable drop, which indicates a loss of stability. In case of flexural failure, this point in time corresponds to the time-step in the calculation in which the prestressing strands at the location of the highest bending moment reach their ultimate strain, indicating a rupture of the steel strands. In case of shear failure, this point in time corresponds to the onset of the formation of large diagonal shear cracks in the webs of the HC slab, which quickly grow larger (indicated as regions of high plastic strain, see Figure 6). This method of defining failure is preferred over the commonly used deflection limits prescribed in EN 1363-1:2012 [23] for flexural tests on concrete members. These deflection limits are based solely on the span of the member and the lever arm of the section and do not take into account the failure mode or the influence of the boundary conditions of the specimen. Fire tests on deep HC slabs [18] have shown that failure (shear-tension) can occur at deflections which are much smaller than those specified as limits during fire tests in EN 1363-1:2012. Similarly, axially restrained concrete members tend to fail at significantly smaller deflections compared to unrestrained members [9].

2.3 VALIDATION

In the following, the performance of the numerical model is validated against the results from experiments reported by Shakya & Kodur [9] and Nguyen et al. [18]. To this end, six fire tests on HC slab members with varying fire scenarios and geometries are modelled. The dimensions, material properties, prestressing, loads and support conditions are modelled to precisely correspond to the reported tests. The cross-section geometry and properties are provided in Figure 1 and Table 1, respectively. The prestressing steel is modelled considering an ultimate strength of 1860 MPa. The test conditions and time-temperature regimes of the fire tests are shown in Table 2 and Figure 2, respectively. By comparing the results from Models 1, 3, 4, 5 and 6 the performance of both the heat-transfer and mechanical models is validated for unrestrained HC exposed to fire. Model 2 is used to validate the model for axially restrained HC slabs exposed to fire, and is based on a validated model for axially restrained HC slabs at ambient temperatures, as presented in Thienpont et al. [3]. In the restrained fire test by Shakya & Kodur, the outward displacement of the HC slab was hindered by two steel tubular sections (203 mm × 203 mm × 12 mm), which were connected by two post-tensioning rods, of 25.4 mm diameter and with an ultimate capacity of 534 kN, installed through the cores of the slab. To simulate this setup in the numerical thermal-stress analysis, the steel sections are modelled by means of two stiff plates at both end of the slab. The post-tensioning rods are modelled as a set of 2-noded linear truss elements. To the knowledge of the authors there are no other well-documented fire tests on restrained HC slabs available in the literature.

Table 1: fire tests used for the validation of the numerical model: geometry and material properties

Model	**Section**	***Span*** ***L*** **[m]**	**Span-to-depth ratio** ***L/h*** **[-]**	**Shear span to effective depth ratio** ***a/d*** **[-]**	**Concrete strength** f_c **[MPa]**	**Area of prestressing steel** A_p **[mm²]**	**Initial prestress** σ_{p0} **[MPa]**	**Ref.**
1	HC200	3.65	18.25	8.93	75	693	1302	[9]
2	HC200	3.65	18.25	8.93	75	693	1302	[9]
3	HC320	4.15	12.97	2.86	54	495	1150	[18]
4	HC400-1	4.15	10.38	2.25	57	1001	1150	[18]
5	HC400-2	2.2	5.5	(*)	54	1386	1150	[18]
6	HC500	4.15	8.3	1.79	56	990	1150	[18]

(*) Heat transfer test only, no loads were applied

Table 2: fire tests used for the validation of the numerical model: fire test conditions

Model	**Section**	**Support conditions**	**Load level [%]**	**Fire scenario**	**Ref.**
1	HC200	simply supported	60	ASTM E119	[9]
2	HC200	restrained	60	ASTM E119	[9]
3	HC320	simply supported	40	Custom I	[18]
4	HC400-1	simply supported	40	Custom II	[18]
5	HC400-2	simply supported	(*)	ISO843	[18]
6	HC500	simply supported	40	Custom I	[18]

(*) Heat transfer test only, no loads were applied

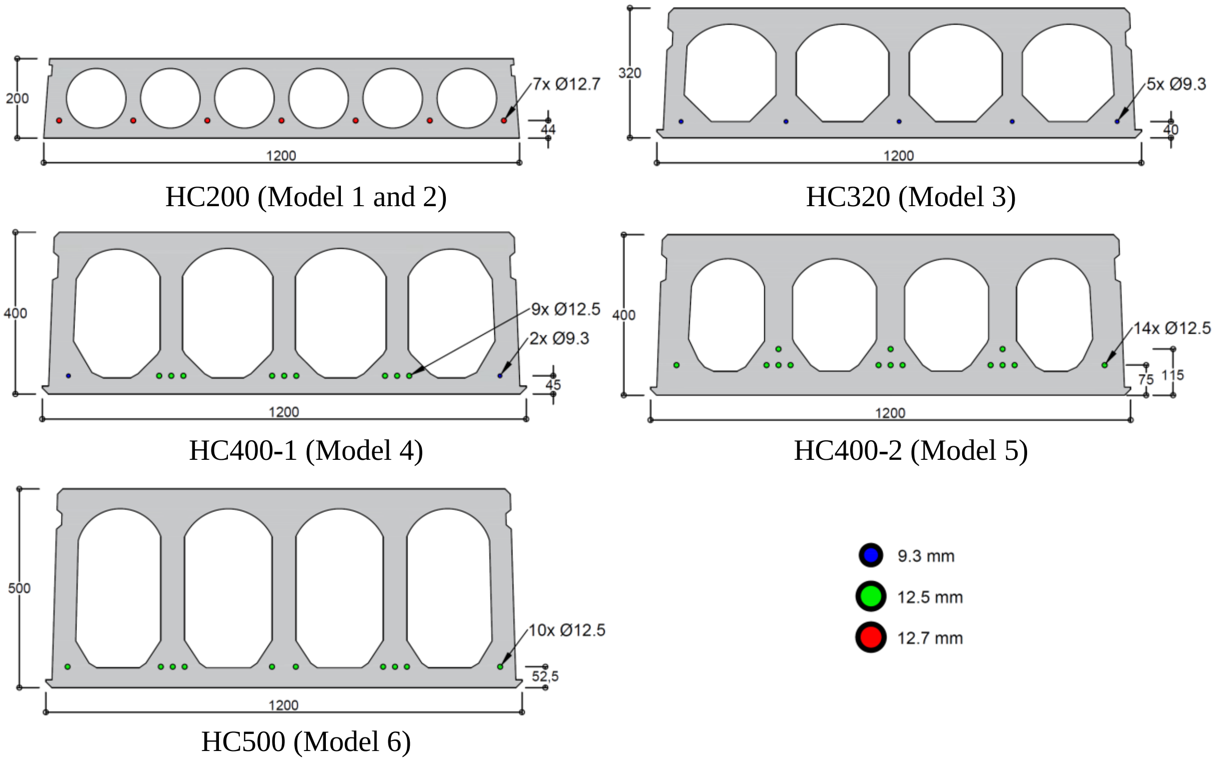

Figure 1: Cross sections of HC slabs used in validation and parametric study (dimensions in mm).

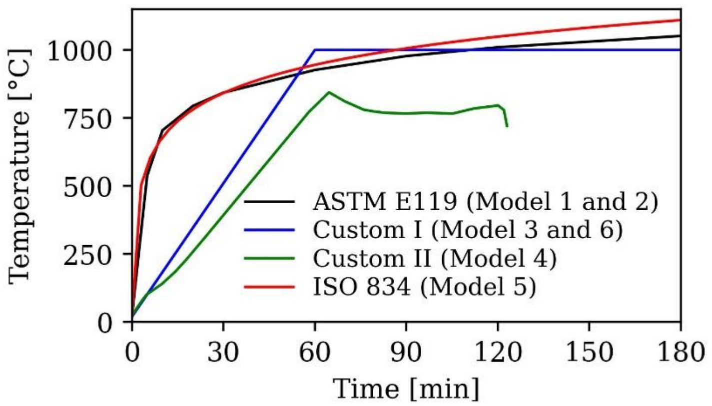

Figure 2: Time-temperature curves of fire tests on HC slabs used in the validation analysis (based on [9,18]).

2.3.1 Thermal heat transfer

Figure 3 depicts the temperatures at various distances from the bottom surface predicted by the heat transfer model alongside the temperatures measured during the fire tests. All experimental temperature measurements were obtained from thermocouples positioned in the centre of the web, i.e., in the middle between two hollow cores. In the numerical model, the temperature values were evaluated at the same locations as in the experiments. It should be noted that the numerical model is not able to fully represent the plateau at 100°C which is observed in the experimental results. This plateau is caused by the vaporization of moisture inside the concrete, which stabilizes the temperature around 100 °C while water content is consumed [24]. Since the heat transfer model does not explicitly account for the full hygrothermal behaviour of fire exposed concrete, this phenomenon is not accurately represented. Other differences between the numerical predictions and the measured temperature values could be attributed to the stochastic nature of the various input variables. For example, concrete has been experimentally observed to show a significant scatter in the values of the thermal conductivity and specific heat, both at room temperature and at the high temperatures typically associated with a building fire [25]. This in turn results in a significant variation in the temperatures inside the concrete section. The latter was also reported by Fellinger [7], who performed a survey of nine fire tests on identical HC sections, and found that the temperature measurements of the strands varied in a range of more than 200 °C after 60 minutes of ISO 834 exposure. Overall, a good correlation between the two sets of temperatures can be observed, illustrating that the heat transfer model can adequately predict the temperature development in HC slabs.

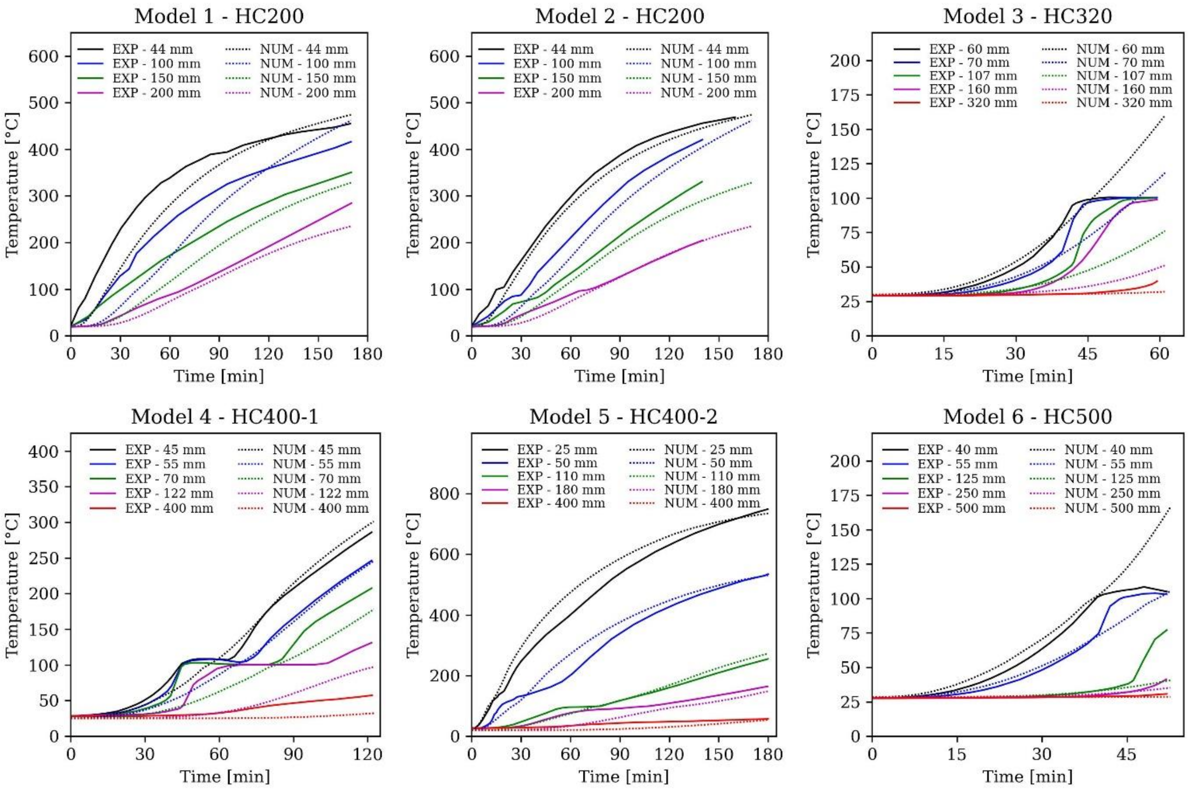

Figure 3: Comparison of temperature development between experiments and numerical model.

2.3.2 Mechanical response

To validate the mechanical response, the numerically predicted crack patterns and mid-span deflections as a function of time are compared with the results from the fire tests. Figure 4 presents the comparison against the unrestrained test (Model 1) and restrained test (Model 2) by Shakya & Kodur [9]. The numerically obtained deflections as a function of time are slightly conservative, but overall the effect of the axial restraint on the time-displacement behaviour is well captured. Furthermore, from the crack patterns shown in Figure 4, it can be concluded that the model is able to correctly predict the failure mode of both fire tests, i.e. flexural cracking for Model 1, and flexural crushing near the middle of the span for Model 2. From a comparison of the results between Model 1 and Model 2, it is clear that restrained thermal expansion positively influences structural response of the considered HC slabs when exposed to fire.

The numerically predicted time-displacement curves and crack patterns at the time of failure for the fire tests (Model 3, 4 and 6) by Nguyen et al. [18] are shown in Figure 5 and Figure 6, respectively. Model 5 is not shown in these figures, as this fire test was performed on an unloaded specimen and only focussed on studying the heat transfer inside the member. As with the previous models, it can be concluded that the model is able to adequately predict the time-displacement behaviour and the failure mode of these specimens (see also Table 3). It is noted that the reported failure mode of model 3 (HC320) was shear tension combined with anchorage failure. The latter failure mode could not be observed in the numerical model due to the previously mentioned perfect bond assumption. Future research investigations will focus on extending the current model with a dedicated bond-slip model.

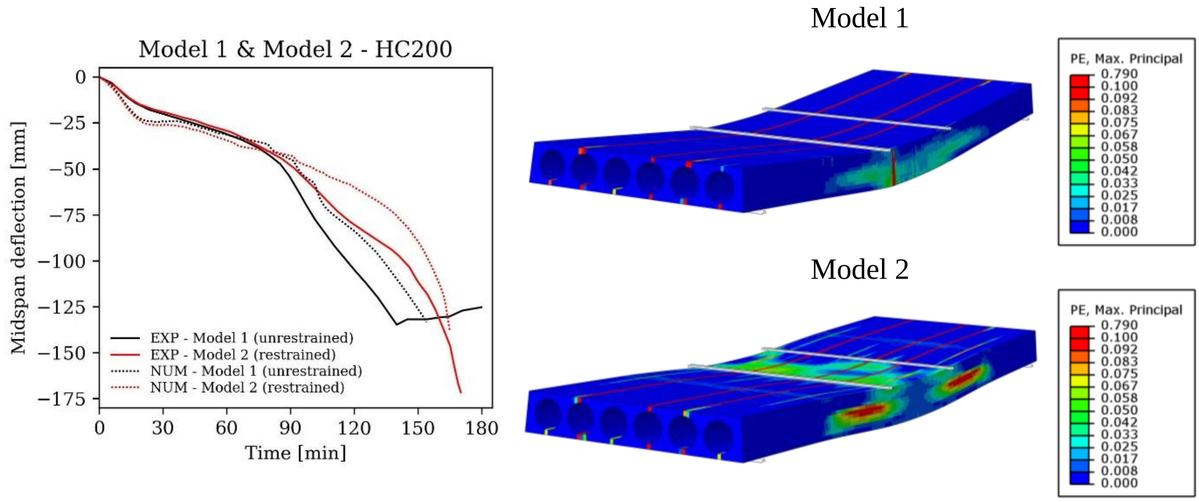

Figure 4: (left) comparison of time-displacement curves between numerical model and tests by Shakya & Kodur [9]; (right) plastic strains plots at the time of failure for Model 1 and 2, indicating cracks (strains in mm/mm)

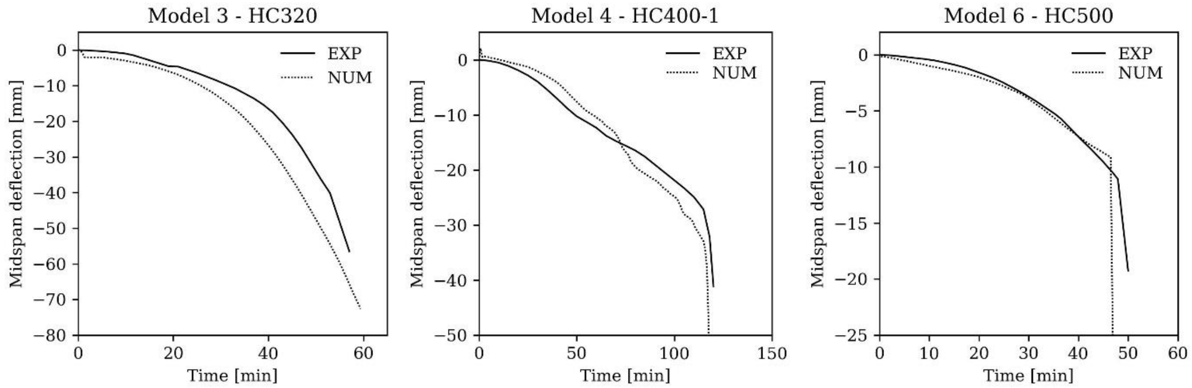

Figure 5: Comparison of time-displacement curves between numerical model and tests by Nguyen et al. [18]

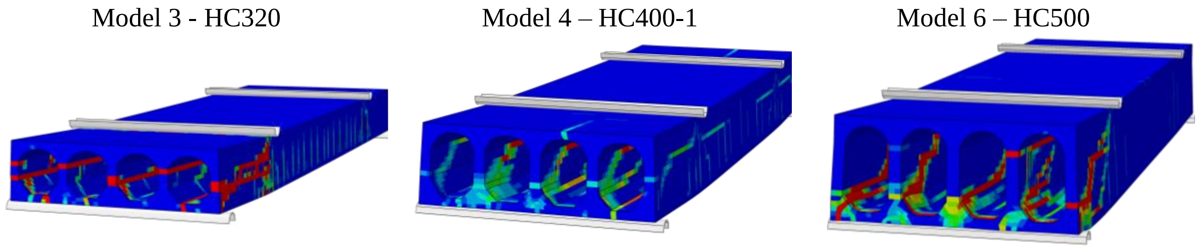

Figure 6: Plastic strains plots at the time of failure for Model 3, 4 and 6, indicating cracks (strains in mm/mm).

Table 3: Validation summary

Model	Section	Failure mode		Failure time [min]		
		EXP	NUM	EXP	NUM	Error
1	HC200	Bending	Bending	140	152	12
2	HC200	Bending	Bending	170	165	5
3	HC320	Web shear & Anchorage	Web shear	57	60	3
4	HC400-1	Web shear	Web shear	118	117	1
5	HC400-2	(*)	(*)	(*)	(*)	(*)
6	HC500	Web shear	Web shear	49	47	2

(*) Heat transfer test only, no loads were applied

3 PARAMETRIC STUDY

In the following, the influence of various degrees of axial restraint on the load-displacement behaviour of concrete HC slabs with realistic span length is investigated. Three HC slab sections, labelled HC200, HC320 and HC500 are evaluated in a restrained four-point bending test setup, as shown in Figure 7. The cross-sectional geometries correspond to those in Figure 1, and the material properties are based on those reported in section 2.3 (see Table 1). In the thermal analyses, the slabs are exposed to the ISO 834 [26] standard time-temperate heating curve at the bottom side, while at the top side ambient conditions are assumed. Prior to the fire exposure, the slabs are preloaded by means of two line loads applied at one-fourth of the span length, up to a certain load level u. The latter is defined as the ratio of the applied loads to a calculated failure load at ambient temperature. For each model, the failure load at ambient temperature is obtained using a validated numerical model for HC slabs presented in [3], using the mean values for the material properties and the geometry.

To simulate the presence of a stiff surrounding structure in a simplified way, the end restraints are modelled by means of two stiff vertical plates connected to springs, with spring stiffness K_{spring}. The rotations of the vertical plates are restricted for all rotational degrees of freedom, and the plates are only allowed to move in the span direction of the slab. In order not to a priori fix the vertical position of the axial restraint force, the interaction between the HC slab ends the stiff plates is modelled with a contact definition. This allows the vertical position of the axial restraint force to change throughout the analysis, as it depends on the rotation at the slab ends. In order to solely investigate the effect of restrained expansion, only the outward displacement, i.e. elongation of the member, is restrained. The springs are modelled to not exert any forces on the member when it moves inwards, beyond its initial position (i.e., its state prior to the fire), as shown in Figure 7. Hence, the formation of catenary action, in which the inward displacements of the slab ends are restrained, is not considered in this study.

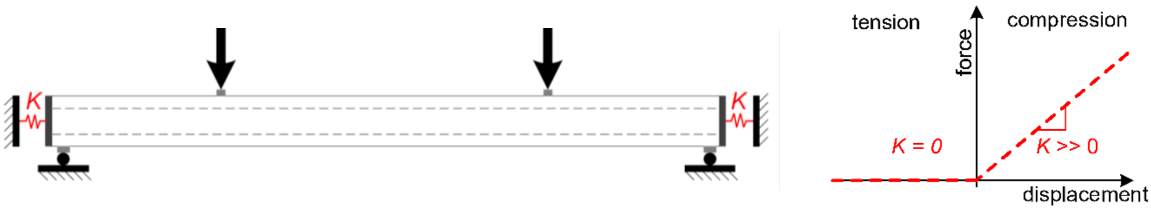

Figure 7: (left) restrained four-point bending setup; (right) schematic force-displacement diagram of the springs

In the figures below, the degree of axial restraint is expressed using a dimensionless factor k, which represents the ratio of the linear spring stiffness K_{spring} to the axial stiffness of the HC slab K_{HC}. The axial stiffness of the slab is calculated as $K_{HC} = E_c \cdot A/L$ (see Table 4), where E_c = the Young's modulus of concrete, L = the span of the member, and A = the effective cross-section of the HC slab. The latter is calculated as the sum of the net cross-sectional area of concrete $A_{c,net}$ and the effective cross-sectional area of the prestressing strands: $A = A_{c,net} + \sum \alpha \cdot A_{p,strand}$, where $\alpha = E_p/E_c$ is the ratio of the Young's Moduli of prestressing steel and concrete.

The structural performance under fire exposure is evaluated in both simply supported conditions ($k = 0$) and for a range of stiffnesses up to $k = 1$ ($K_{spring} = K_{HC}$). It can be noted that the upper end of this stiffness range is very high, and that it is doubtful that such a level of restraint could occur in a real building. The forces involved are so high, that large displacements in the adjacent members will likely occur, and that movement will be accompanied by a large reduction in the restraining force [27]. Non-linear springs could be used to model a more complex response of the surrounding structure, but such approach is considered outside the scope of this work.

Table 4: Axial stiffness K_{HC} of the HC slabs in the parametric study for various span-to-depth ratios *L/h* (in kN/mm)

Section	L/h = 25	L/h = 30	L/h = 35
HC200	1070.6	895.1	769.0
HC320	692.6	578.4	496.5
HC500	616.7	514.5	441.5

3.1 CRACK PATTERNS AND FAILURE MODES

Depending on the degree of axial restraint, different crack patterns are observed in the evaluated HC slab specimens. In unrestrained slabs, and slabs with a low degree of axial restraint, large vertical cracks are observed in the webs of the HC slabs, at regular distances (see Figure 8a). These cracks have also been observed experimentally [7,18], and originate from the non-linear temperature field over the depth. and the corresponding thermal strains in the axial direction, which vary non-linearly over the depth of the slab. In order to maintain compatibility of the total strain over the depth of the slab in the axial direction, mechanical strains have to develop to counteract these incompatible thermal strains, which leads to cracking in the middle of the section [28]. When the degree of axial restraint increases, the size of these cracks decreases [5], and for cases of very high axial restraint, no vertical cracks are observed. In line with experimental observations by Fellinger [7], these vertical cracks do not necessarily lead to failure of the HC slab.

From the numerical evaluations, two types of failure modes are observed. When the degree of axial restraint is small, the HC slabs generally tend to fail in bending, after rupture of the prestressing strands at the location of the highest bending moment. Conversely, when the stiffness of the surrounding structure is higher, shear tension failure is observed in the webs of the HC slab. As a result of the restrained thermal expansion at the slab ends, large compressive forces develop in the cross section, which lead to an altered stress state in the webs of the HC slabs. When the tensile stresses in the web exceed the admissible concrete tensile strength, shear cracks develop inside the webs, which extend from the support to the load-application point. As the webs of HC slabs typically don't contain any transverse reinforcement, the slab fails immediately after the formation of these shear cracks. The crack patterns of both types of failure are illustrated in Figure 8, for a HC320 section with a span of 8 m.

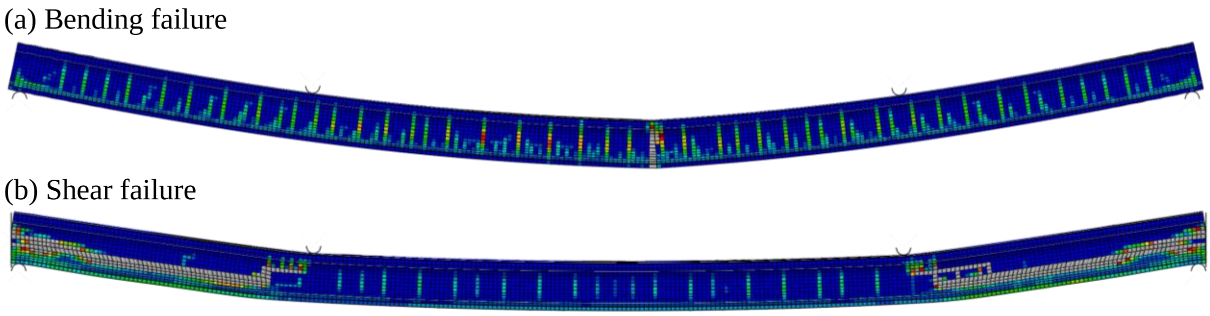

Figure 8: Failure modes of restrained HC slabs exposed to fire, plastic strains plots indicating cracks (strains in mm/mm)

3.2 Influence of axial restraint stiffness

In the following, the influence of the degree of axial restraint on the time-displacement behaviour and failure mode of fire exposed HC slabs is evaluated. Each of the studied specimens has a span-to-depth ratio of L/h = 25, and an applied load corresponding to 30% of the ambient capacity (load level u = 30%). Similar to the models described in Section 2, in these evaluations failure is defined as the point in time where the slab can no longer carry the applied loads.

As shown in Figure 9, the fire resistance time of type HC200 members decreases significantly in the lower range of restraint stiffness values ($0 < k < 0.4$). This reduction in failure time is potentially caused by the failure mode, which changes from flexural bending to a premature shear tension failure when the thermal expansion is restrained. For higher restraint stiffnesses ($k \geq 0.4$) however, a significant increase in failure time, up to 60 minutes, can be observed. This increase could be attributed to the large restraint forces which develop inside the member. These large restraint forces result in high compressive stresses inside the webs in the longitudinal direction of the member, which prevent the formation of vertical cracks. As the fire exposure progresses, the material properties in the bottom flange start to decay, which eventually leads to crushing of the concrete near the supports and reduced restraint forces.

The results for the HC320 and HC500 section are shown in Figure 10 and Figure 11 respectively. For both types of slabs, the fire resistance time increases significantly when the axial thermal expansion is restrained. In the range of relatively low axial restraint stiffnesses ($0 < k < 0.1$), the fire resistance time rapidly increased with the degree of axial restraint. For higher degrees of axial restraint ($k > 0.1$), the failure mode changes from bending to shear tension, and the additional gain in failure time tends to level out. Unlike the HC200 slabs, in which restrained thermal expansion only improves the fire resistance in highly restrained cases, these taller HC slabs always benefit from the presence of axial restraint; restrained thermal expansion always leads to an increased fire resistance time, regardless of the degree of restraint.

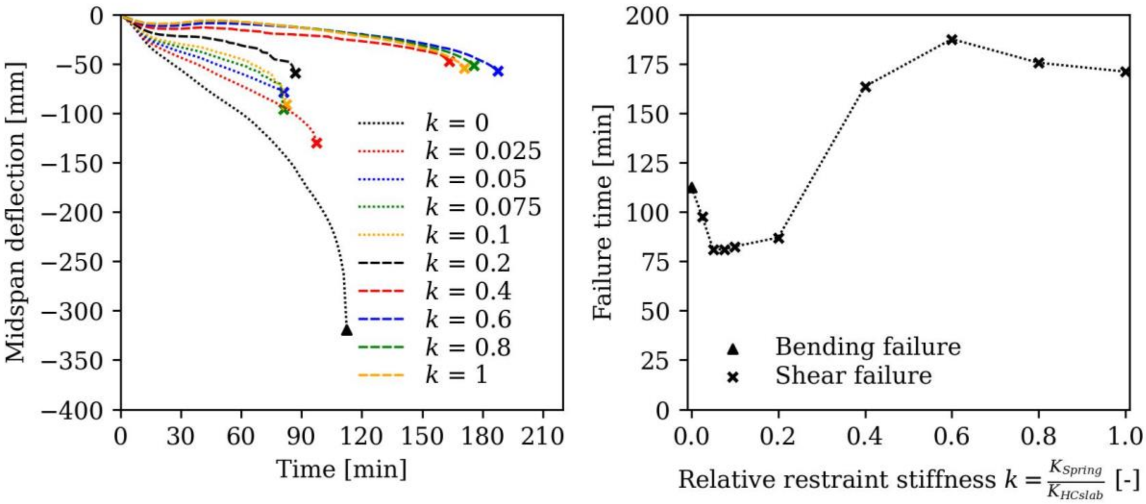

Figure 9: Influence of axial restraint stiffness on the fire resistance of HC200, span length 5.0 m, load level 30%: (left) time displacement curves; (right) failure time and failure mode

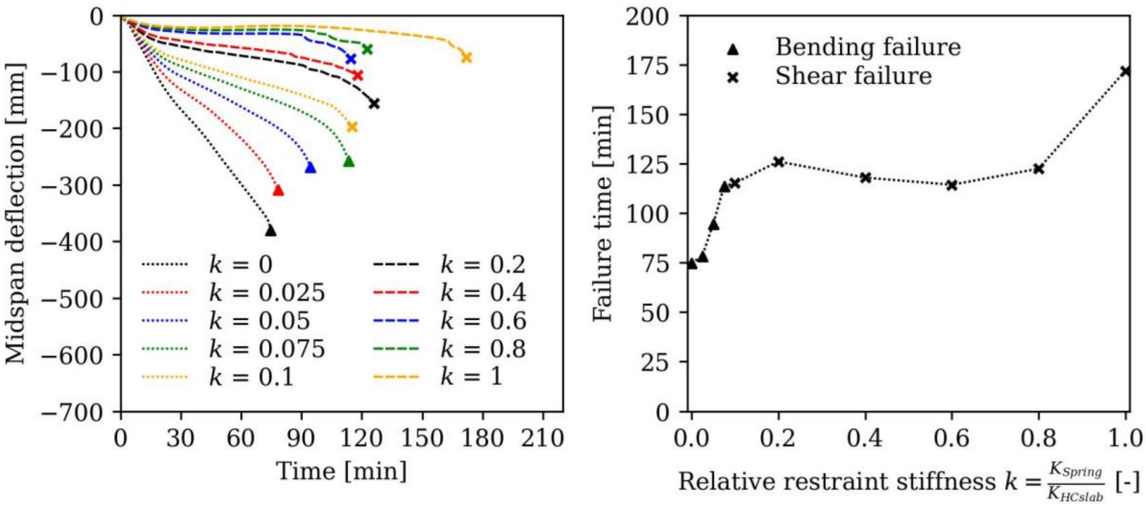

Figure 10: Influence of axial restraint stiffness on the fire resistance of HC320, span length 8.0 m, load level 30%: (left) time displacement curves; (right) failure time and failure mode

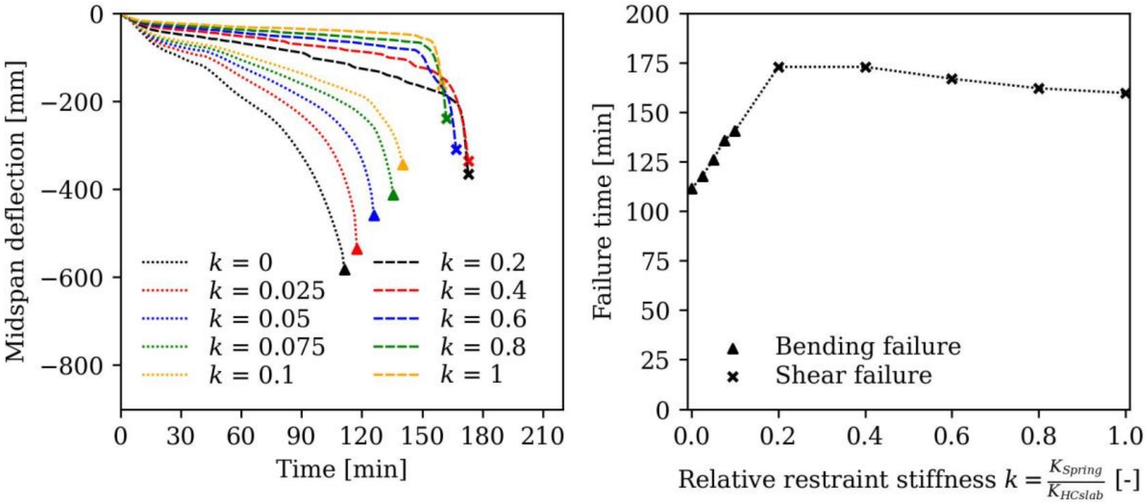

Figure 11: Influence of axial restraint stiffness on the fire resistance of HC500, span length 12.5 m, load level 30%: (left) time displacement curves; (right) failure time and failure mode

3.3 INFLUENCE OF OTHER PARAMETERS

In a next set of analyses, the influence of the span-to-depth ratio L/h, the utilization ratio u, the concrete compressive strength f_c and the initial prestress σ_{p0} are investigated. Firstly, to study the influence of the span-to-depth ratio, three values are considered: $L/h = 25$, $L/h = 30$ and $L/h = 35$, see Figure 12. From the graphs, it is clear that a higher span-to-depth ratio ($L/h \geq 30$) almost always leads to a reduced fire resistance time for axially restrained HC slabs. This reduced failure time could be attributed to the larger deflections which occur in more slender members when they are exposed to fire from the bottom. These deflections lead to the development of the second order moments due to the P-Δ effect (the axial restraint force P, and vertical deflection Δ, will develop a second order moment in the member) of the axial restraint force. These second order moments cause the deflections to grow even larger, which eventually leads to early failure of the member. In some cases (e.g. in HC320 slabs with a 9.6 m span and $k \geq 0.2$, see Figure 12.b) the restraint forces are large enough to prevent the formation of large deflections and to some extent CAA can develop. For very high span-to-depth ratios ($L/h = 35$) even the highest degree of axial restraint does not lead to an improved fire resistance. It is concluded that the beneficial effect of restrained thermal expansion which is typically observed in lab scale fire tests can also occur in HC slabs with realistic span lengths, except for cases with very high span-to-depth ratios, where the beneficial effect is counteracted by second order moments. Lastly, Figure 12 also illustrates a lower failure time of the HC320 slab compared to the HC200 slab, in case of unrestrained boundary conditions

($k = 0$). Since both members fail in bending, this difference can be explained by the rebar axis distance of the prestressing strands, which is smaller in HC320 section (40 mm), compared to the HC200 section (44 mm). Hence, when exposed to fire, the prestressing strands in the HC320 section will heat up and loose strength faster compared to the strands in the HC200 section.

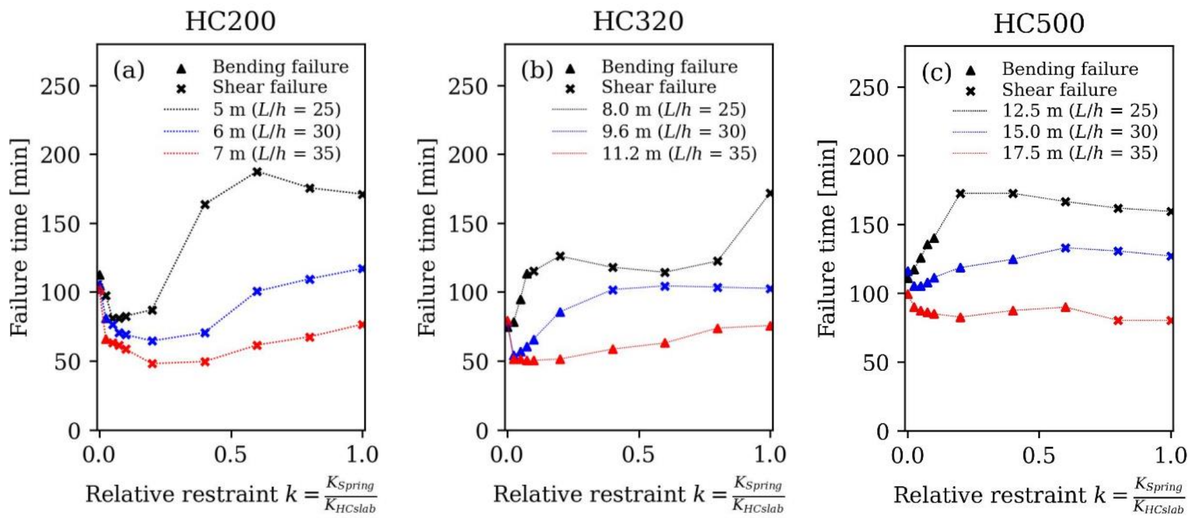

Figure 12: Influence of span-to-depth ratio L/h on the fire resistance of axially restrained HC slabs, load level 30%: (a) HC200; (b) HC320; (c) HC500

Next, the influence of the load level is investigated in Figure 13, for values ranging from 20% to 40%. In each graph, the results are obtained for HC200, HC320 and HC500 sections with a span-to-depth ratio $L/h = 30$. From the graphs, it is clear that the load-ratio strongly influences both the fire resistance time and failure mode. This is especially true for the case of the HC200 slab with a load level $u = 40\%$.

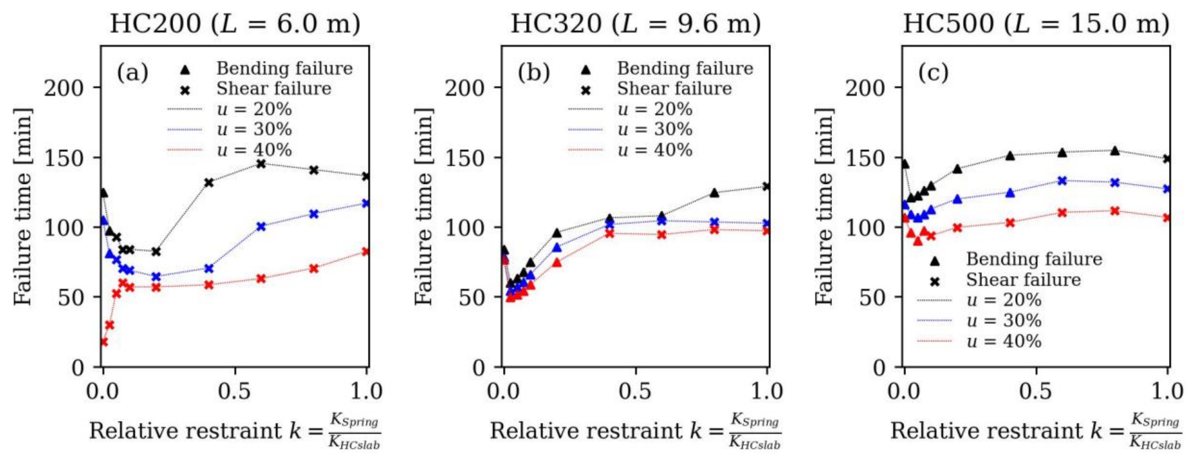

Figure 13 Fire resistance and failure mode of restrained HC slabs, span-to-depth ratio $L/h = 30$, load levels $u = 20\%$, 30% and 40%: (a) HC200; (b) HC320; (c) HC500

In a last set of analyses, the influence of the concrete compressive strength f_c, concrete tensile strength f_{ct} and initial prestress in the prestressing strands σ_{p0} is investigated, see Figure 14. The graphs clearly illustrate that these parameter have far less influence of the fire resistance time, when compared to the span length, load level and degree of axial restraint. Only in case of the initial prestress, a slight improvement in the fire resistance time is noted, for cases with a higher initial prestress. This enhanced fire resistance could be attributed to the higher compressive forces inside the section, which prevent the formation of vertical cracks in the webs.

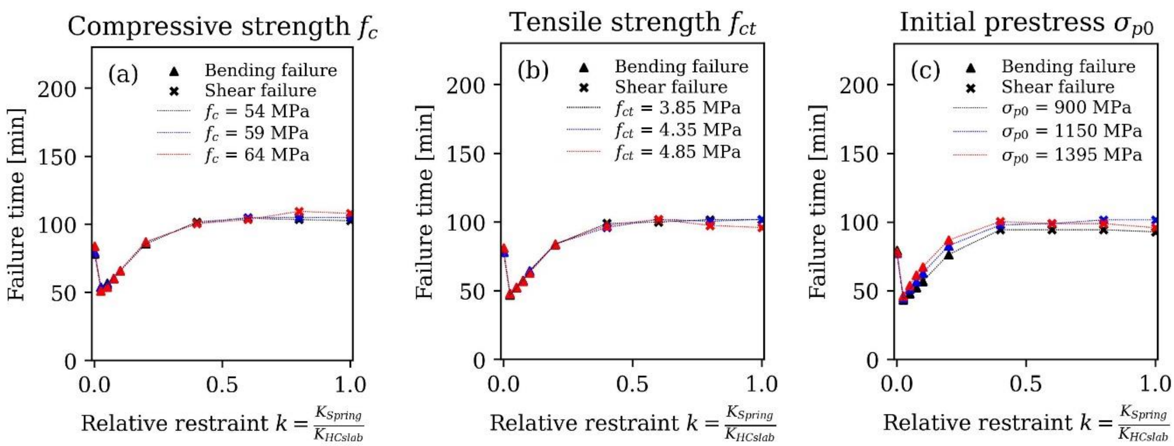

Figure 14: Fire resistance and failure mode of restrained HC320 slabs, span-to-depth ratio *L/h* = 30, load level *u* = 30%: influence of (a) concrete compressive strength f_c; (b) concrete tensile strength f_{ct}; (c) initial prestress σ_{p0}

4 DISCUSSION

To date, the influence of axial restraints on the structural performance of HC slabs exposed to fire has rarely been studied. The present contribution established a numerical model that can predict the fire resistance and failure mode of HC with restrained boundary conditions, and is intended as a first stepping stone toward gaining a thorough understanding of this phenomenon in hollow core floor systems. In the following, some remarks with regard to the presented numerical evaluations are discussed, as well as the identified research needs.

Thus far, only a limited number of experimental fire tests have been performed on HC with restrained boundary conditions. Moreover, to the knowledge of the authors, no restrained fire tests have been performed on deep HC slabs (i.e. slabs with a depth larger than 200 mm), nor on members with large (realistic) span lengths. Additional tests are required to further validate the presented results for deep HC slabs exposed to fire, and the expected change in failure mode in the presence of axial restraints.

In the numerical model evaluations, the restraining boundary conditions are a simplification of the boundary conditions that are typically occurring in practice. Performing similar evaluations on restrained HC slabs of which the slab ends are connected to a realistic surrounding structure (e.g., a cast in place concrete beam) would introduce numerous additional complexities, and the possibility of a local failure in the region of the supports. In this study, the main focus is on the structural behaviour of an isolated HC slab member. Nonetheless, in a follow-up study, a more realistic modelling of the boundary conditions would be relevant. Moreover, in this contribution, only the restraint stiffness in the longitudinal direction is considered. However, in practice a certain degree of lateral (sideways) restraint is likely to be present as well, which could affect the stress state and structural performance [7].

Lastly, the current contribution only considers the structural behaviour of HC slabs exposed to the standardized ISO 834 time-temperature curve. Herein, the temperature rise is defined as monotonically increasing. Although tests based on this predefined time-temperature curve provide a standardized way of comparing the performance of structural members exposed to fire, the performance-based analysis of the structural behaviour in a realistic fire scenario would be a relevant extension to the research. Such a realistic fire scenario is not only characterized by a heating phase, but also by a cooling phase, in which the temperature in the compartment decreases back to ambient conditions [14,29]. A thorough study on the influence of natural fires and the structural performance during and after the cooling will be incorporated in future research investigations.

5 CONCLUSIONS

The structural behaviour and fire resistance of fire exposed precast concrete hollow core (HC) slabs can be strongly affected when the thermal expansion at the slab ends is restrained by a stiff surrounding structure. Previous investigations into this topic have primarily focused on shallow HC slabs with short span lengths, mainly due to the size limitations of test furnaces. Therefore, this contribution studies this effect on the fire resistance and failure mode of both shallow and deep HC slabs with real-scale dimensions, by means of a numerical model. The main conclusions are reported in the following:

- Despite the large number of fire tests on HC slabs reported in the literature, only a fraction of these tests were performed on restrained members. To date the influence of restrained thermal expansion in deep HC slabs has not yet been studied in an experimental setup.
- The proposed finite element based numerical model is capable of adequately predicting the structural performance of HC slabs in restrained and unrestrained conditions. More tests on restrained HC slabs are needed to further validate the performance of the model.
- The numerical results demonstrate that restrained thermal expansion significantly influences the structural behaviour of fire exposed HC slabs with real-scale span lengths, even for relatively small degrees of axial restraint. The effects are present in all investigated HC sections, ranging from shallow 200 mm slabs to deep HC slabs with a depth up to 500 mm. Depending on the axial restraint stiffness and the span-to-depth ratio, restrained thermal expansion of precast HC slabs can either lead to a significantly enhanced fire resistance time, or a severe reduction of the time to failure. In the former case, which mainly occurs in HC slabs with small span-to-depth ratios, restrained thermal expansion can lead to an enhancement of the fire resistance with up to 60 minutes, compared to a simply supported slab. This enhanced fire resistance can be attributed to the formation of compression arching action in the webs of the HC slab, and an enhanced shear behaviour caused by the large axial restraint force. Conversely, in the latter case, which mainly occurs in HC slabs with high span-to-depth ratios, restrained thermal expansion is shown to lead to a substantial reduction of the fire resistance time, up to 30 minutes compared to a simply supported slab. This reduction in fire resistance time can be attributed to the development of second order moments at the slab ends and/or a change in the failure mode.
- From the parametric study, the degree of axial restraint, the span-to-depth ratio and load level are identified as the most influential parameters with regard to the ultimate capacity and failure mode of restrained HC slabs.
- The results highlight that numerical analysis is required to evaluate the effect of restraint on the fire resistance of hollow core slabs, and that in general the restraint cannot readily be assumed to have a positive, or negative, effect on the fire resistance rating.

ACKNOWLEDGEMENTS

The authors wish to thank the Research Foundation of Flanders (FWO) for the financial support on the research project (Grant number 11F5520N) “Performance-based analysis and design for enhancing the safety of prestressed concrete hollow-core slabs in case of fire and un- foreseen events”. The computational resources (Stevin Supercomputer Infrastructure) and services used in this work were provided by the VSC (Flemish Supercomputer Center), funded by Ghent University, FWO and the Flemish Government – department EWI.

REFERENCES

[1] K.S. Elliott, C. Jolly, Multi-storey Precast Concrete Framed Structures, Wiley, Oxford, UK, 2016. https://doi.org/10.1002/9781118587379.

[2] A. Van Acker, S. Maas, Historical development of Hollow Core slabs, Concr. Plant Int. 2 (2021) 142–153.

[3] T. Thienpont, W. De Corte, R. Van Coile, R. Caspeele, Compressive membrane action in axially restrained hollow core slabs : Experimental investigation, Struct. Concr. (2022) 1–14. https://doi.org/https://doi.org/10.1002/suco.202100684.

[4] C.C. Carlson, S.L. Selvaggio, A.H. Gustaferro, A review of studies of the effects of restraint on the fire resistance of prestressed concrete, Portl. Cem. Assoc R D Lab Bull. (1965).

[5] J.-C. Dotreppe, J. Franssen, Precast hollow core slabs in fire: numerical simulations and experimental tests, in: Proc. SiF’04 Third Int. Struct. Fire Work., Ottawa, 2004: pp. 219–232.

[6] J.-C. Dotreppe, P.F. Bisschops, L. Mievis, J.-M. Franssen, Programme d’appui à la normalisation nationale et européenne en sécurité incendie, (1998).

[7] J. Fellinger, Shear and anchorage behaviour of fire exposed hollow core slabs (PhD Thesis), Technische Universiteit Delft, 2004.

[8] J. Fellinger, J. Stark, J. Walraven, Shear and anchorage behaviour of fire exposed hollow core slabs, Heron. 50 (2005) 279–301.

[9] A.M. Shakya, V.K.R. Kodur, Response of precast prestressed concrete hollowcore slabs under

fire conditions, Eng. Struct. 87 (2015) 126–138. https://doi.org/10.1016/j.engstruct.2015.01.018.

[10] V.K.R. Kodur, A.M. Shakya, Factors governing the shear response of prestressed concrete hollowcore slabs under fire conditions, Fire Saf. J. 88 (2017) 67–88. https://doi.org/10.1016/j.firesaf.2017.01.003.

[11] K. LaMalva, L. Bisby, J. Gales, T. Gernay, E. Hantouche, C. Jones, A. Morovat, R. Solomon, J. Torero, Rectification of "restrained vs unrestrained," Fire Mater. 44 (2020) 341–351. https://doi.org/10.1002/fam.2771.

[12] V.K.R. Kodur, M. Dwaikat, Effect of fire induced restraint on fire resistance of reinforced concrete beams, J. Struct. Fire Eng. 1 (2010) 73–88. https://doi.org/10.1260/2040-2317.1.2.73.

[13] Dassault Systemes, Abaqus 6.14: Abaqus/CAE User's Guide, (2014).

[14] T. Thienpont, R. Van Coile, R. Caspeele, W. De Corte, Burnout resistance of concrete slabs: Probabilistic assessment and global resistance factor calibration, Fire Saf. J. 119 (2021) 103242. https://doi.org/10.1016/j.firesaf.2020.103242.

[15] M.B. Dwaikat, V.K.R. Kodur, A numerical approach for modeling the fire induced restraint effects in reinforced concrete beams, Fire Saf. J. 43 (2008) 291–307. https://doi.org/10.1016/j.firesaf.2007.08.003.

[16] R. Van Coile, Reliability-Based Decision Making for Concrete Elements Exposed to Fire (PhD thesis), Ghent University, 2015.

[17] A.H. Buchanan, A.K. Abu, Structural design for fire safety, John Wiley & Sons, 2017.

[18] H.T.N. Nguyen, K.H. Tan, Shear response of deep precast/prestressed concrete hollow core slabs subjected to fire, Eng. Struct. 227 (2021) 111398. https://doi.org/10.1016/j.engstruct.2020.111398.

[19] CEN, EN 1992-1-2. Eurocode 2 – design of concrete structures. Part 1–2: general rules – structural fire design, Brussels, 2004.

[20] CEN, EN 1991-1-2. Eurocode 1: actions on structures – Part 1–2: general actions – actions on structures exposed to fire., Brussels, 2002.

[21] fib, fib Model Code 2010, Final draft – Volume 1, Com. Euro- Int. Du Bét. (2012). http://repositorio.unan.edu.ni/2986/1/5624.pdf.

[22] S. Albrifkani, Y.C. Wang, Explicit modelling of large deflection behaviour of restrained

reinforced concrete beams in fire, Eng. Struct. 121 (2016) 97–119. https://doi.org/10.1016/j.engstruct.2016.04.032.

[23] CEN, Fire Resistance Tests–Part 1: General Requirements (EN 1363-1: 2012), Brussels, 2012.

[24] J. V. Aguado, V. Albero, A. Espinos, A. Hospitaler, M.L. Romero, A 3D finite element model for predicting the fire behavior of hollow-core slabs, Eng. Struct. 108 (2016) 12–27. https://doi.org/10.1016/j.engstruct.2015.11.008.

[25] B. Jovanović, N.E. Khorasani, T. Thienpont, R.K. Chaudhary, R. Van Coile, Probabilistic models for thermal properties of concrete, in: Proc. 11th Int. Conf. Struct. Fire, The University of Queensland, Brisbane, Australia, 2020: pp. 342–352. https://doi.org/10.14264/363ff91.

[26] International Organization for Standardization, ISO 834-1975. Fire resistance tests- elements of building construction, 1975.

[27] A.H. Gustaferro, Design of Prestressed Concrete for Fire Resistance., J Prestress. Concr Inst. 18 (1973) 102–116. https://doi.org/10.15554/pcij.11011973.102.116.

[28] Comité Euro- International du Béton, fib Bulletin 46: Fire Design of concrete structures – structural behaviour and assessment, 2008.

[29] T. Gernay, J.M. Franssen, A performance indicator for structures under natural fire, Eng. Struct. 100 (2015) 94–103. https://doi.org/10.1016/j.engstruct.2015.06.005.